Misfit-dislocation generation by dissociated dislocations in quantum-well heterostructures

J. Zou and D. J. H. Cockayne
Electron Microscope Unit, The University of Sydney, Sydney, New South Wales 2006, Australia
(Received 26 April 1993)

The mechanisms whereby 60° misfit dislocations are generated from dissociated threading dislocations in quantum-well heterostructures are considered. The two partial dislocations experience different misfit stresses, resulting in each partial having a different critical thickness. As a consequence, a number of different dislocation configurations are predicted, including the possibility of producing stacking faults of infinite width.

I. INTRODUCTION

Strained-layer heterostructures have received considerable attention due to their electronic and optoelectronic properties. When a strained layer is grown on a substrate, coherent growth is obtained up to a critical thickness. With continued growth, misfit dislocations are generated to relieve the misfit strain of the heterostructure. Misfit dislocations in strained-layer heterostructures are important because they influence electronic and optoelectronic properties of the heterostructures. To determine critical thicknesses, several theories have been developed.[1-15] Most of them are based on perfect misfit dislocations. However, it is well known that, in bulk semiconductor materials, perfect glide dislocations generally dissociate into two partials that are separated by a stacking fault.[16] Moreover, it has been shown that, in low strain heterostructures, misfit dislocations are dissociated.[17]

The generation of single partial misfit dislocations in single heterostructures has been discussed by several authors,[3,5,8,9] and Hwang and co-workers[18,19] have considered the generation of single partial misfit dislocations in quantum-well heterostructures. However, because threading dislocations and misfit dislocations are dissociated,[17,20] misfit dislocation generation by a pair of partial dislocations must be considered for any accurate theoretical treatment. In our recent theoretical investigation,[20] the particular case of misfit dislocation generation by dissociated dislocations in single heterostructures with [001] growth direction is discussed for isotropic media. Since semiconductors are anisotropic, the effect from anisotropic media must be taken into account. In this paper, the general case of the misfit dislocation generation mechanisms from dissociated threading dislocations and of the critical thicknesses of partial misfit dislocation generations in quantum-well heterostructures are considered theoretically using anisotropic elasticity theory.

II. THEORETICAL CRITICAL THICKNESSES OF DISSOCIATED DISLOCATIONS IN SINGLE QUANTUM-WELL HETEROSTRUCTURES

Matthews and Blakeslee[4] suggested that the generation mechanism of misfit dislocations in epitaxial multilayers is the extension of one-half misfit dislocation loops formed from pre-existing undissociated threading dislocations. This occurs if the strained-layer thickness exceeds the critical thickness of misfit dislocation loop generation, and results in misfit dislocations lying at the two interfaces. They determined the critical thickness by considering two forces,[4] the driving force arising from the misfit strain and the frictional force due to the dislocation line tension at the two strained interfaces.

Jesser and Fox[12,13] suggested that the misfit dislocation generation from a pre-existing threading dislocation is resisted by the static Peierls force and by decoration pinning. Our previous studies[21,22] of GaAs/$In_xGa_{1-x}As$/GaAs single quantum-well heterostructures have shown that the misfit dislocations loops are generated from pre-elongated threading dislocations in the strained interface of the strained layer and the substrate. These studies indicate that, for these pre-elongated threading dislocations, there is no decoration pinning effect on the misfit dislocation loop generation. Further, if the misfit dislocation elongation is controlled by the kink motion, the static Peierls force is not a consideration. For these reasons, the two forces proposed by Jesser and Fox[12,13] are not considered here.

However, if the pre-elongated threading dislocations are dissociated, two additional forces must be considered: the force required to reduce or increase the stacking fault width between two partial dislocations, and the repulsive force between the two partials. Therefore, there are four forces acting on each partial as shown in Fig. 1. These four forces are as follows.

(1) The driving force

$$F_\varepsilon = Mb_p \cos\theta_1 \varepsilon h \ , \tag{1}$$

where b_p, h, and θ_1 are the magnitude of the Burgers vector of the partial dislocation, the strained-layer thickness, and the angle between the Burgers vector and that direction in the interface which is perpendicular to the intersection line of the glide plane and the interface, respectively. ε is the misfit strain in the strained layer, which is equal to the lattice mismatch f if there is no misfit dislocation in the heterostructure. M [$=M(hkl)$] is the biaxial elastic modulus of the strained layer (see the Appendix).

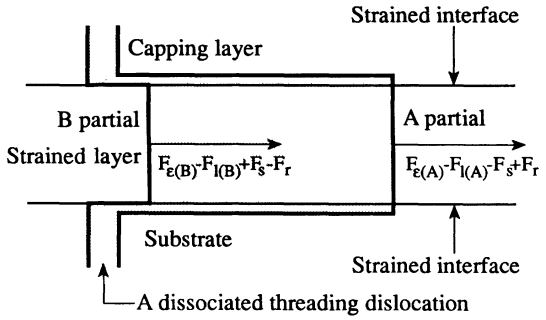

FIG. 1. Schematic diagram of the misfit dislocation generation from a dissociated threading dislocation in single quantum-well heterostructures. Four forces acting on each partial in the strained layer are shown.

(2) The frictional force arising from the dislocation line tension at the two strained interfaces[23]

$$F_1=\frac{K(\theta)b_p^2}{2\pi}\ln\left[\frac{\alpha h}{b_p}\right], \tag{2}$$

where $K(\theta)$ is the energy coefficient depending upon θ, the angle between the Burgers vector of the partial and its line direction.[23] [It is to be noted that $K(\theta)$ differs very little from its isotropic approximation. For GaAs, this difference is less than 3%. For this reason, the isotropic formula of Eq. (2) can be used for simplicity. In the isotropic media,

$$K(\theta)=\frac{\mu(1-\nu\cos^2\theta)}{(1-\nu)},$$

where μ and ν are the shear modulus and Poisson's ratio of the strained layer.] α is the dislocation core factor [for semiconductor materials, α is in the range of 2–4 (Refs. 9, 18, 19, 21, and 22)].

(3) The force required to change the stacking fault width[3,5,8,9]

$$F_s=\frac{\gamma h}{\cos\theta_2}, \tag{3}$$

where γ is the stacking fault energy and θ_2 is the angle between the normal to the glide plane and that direction in the interface that is perpendicular to the intersection line of the glide plane and the interface.

(4) The repulsive force between the two parallel partials is[24]

$$F_r=\frac{Bb_p^2h}{\Gamma\cos\theta_2}, \tag{4}$$

where Γ is the distance between the two parallel partials. In the isotropic media,

$$B=\frac{\mu(2-\nu)}{8\pi(1-\nu)}\left[1-\frac{2\nu\cos2\theta'}{2-\nu}\right],$$

where θ' is the angle between the Burgers vector of the perfect dislocation segment in the strained layer and its line direction. Following Hirth and Lothe,[23] B can be derived also for the anisotropic case, but as for $K(\theta)$, the difference from the isotropic form of Eq. (4) is negligible.

The excess forces acting on the leading (A) partial and on the trailing (B) partial are $F_{\text{exc}(A)}=F_{\varepsilon(A)}-F_{1(A)}-F_s+F_r$ and $F_{\text{exc}(B)}=F_{\varepsilon(B)}-F_{1(B)}+F_s-F_r$, respectively. Therefore, the critical thicknesses at which the A partial misfit dislocation loop will extend in the two interfaces and at which the B partial misfit dislocation loop will extend can be obtained from the conditions

$$F_{\text{exc}(A)}=F_{\varepsilon(A)}-F_{1(A)}-F_s+F_r=0, \tag{5a}$$

$$F_{\text{exc}(B)}=F_{\varepsilon(B)}-F_{1(B)}+F_s-F_r=0, \tag{5b}$$

which give

$$H_c(\theta,\Gamma)=\frac{K(\theta)b_p^2}{2\pi\left[Mb_p\cos\theta_1\varepsilon\mp\dfrac{\gamma}{\cos\theta_2}\pm\dfrac{Bb_p^2}{\Gamma\cos\theta_2}\right]\times\ln\left[\dfrac{\alpha H_c(\theta,\Gamma)}{b_p}\right]}, \tag{6}$$

where the upper sign corresponds to the leading partial and the lower sign corresponds to the trailing partial. This equation is a general equation for the critical thickness of partial misfit dislocation generation. [In this paper, we use the terminology $H_c(\theta,\Gamma)$ to denote the critical thickness for the θ partial when the dissociation width is Γ.]

We assume that, before elongating at the strained interface, the dissociation width of threading dislocations has the equilibrium value Γ_0, and that the misfit strain is equal to the lattice mismatch (i.e., $\varepsilon=f$). This implies that $F_s=F_r$ in Eqs. (5a) and (5b), and so Eq. (6) with $\varepsilon=f$ gives the critical thickness for both partials separately as

$$H_c(\theta,\Gamma_0)=\frac{K(\theta)b_p}{2\pi M\cos\theta_1\varepsilon}\ln\left[\frac{\alpha H_c(\theta,\Gamma_0)}{b_p}\right], \tag{7}$$

where $K(\theta)$ and θ_1 refer to the individual partials.

Because glide misfit dislocations in strained-layer heterostructures are generally 60° dislocations,[21,22] we consider a 60° perfect dislocation dissociated into a 30° partial and a 90° partial. The critical thicknesses of the 30° partial and the 90° partial, given by Eq. (7), for the [001], the [111], and the [110] growth directions, are plotted in Fig. 2 as a function of f, where the anisotropic parameters of GaAs [$M(hkl)$ see the Appendix, $K(30°)=4.84\times10^{10}$ N/m^2, and $K(90°)=6.19\times10^{10}$ N/m^2] and $\alpha=e=2.72$ are used. Figure 2 shows that, for all three growth directions, $H_c(90°,\Gamma_0)<H_c(30°,\Gamma_0)$, indicating that the 90° partial will start to elongate before the 30° partial. When this occurs, Γ changes, so that the critical thickness for the 30° partial, as given by Eq. (6), changes. It is clear that this is so, because since Γ changes, the repulsive force between the two partials changes.

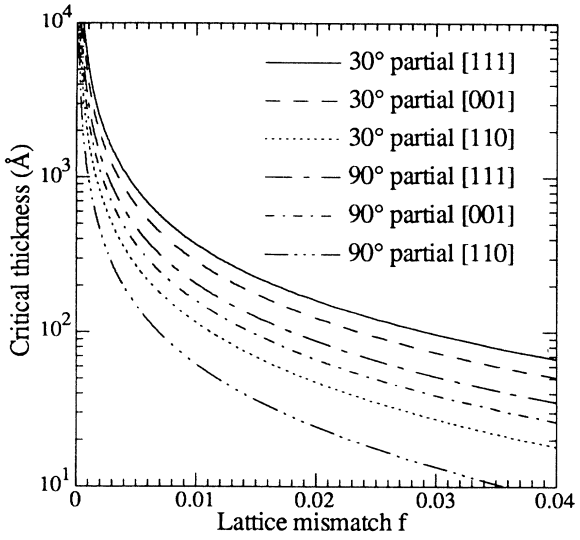

FIG. 2. Plots of the critical thicknesses of the 30° partial dislocation and the 90° partial dislocation [using Eq. (7)] as a function of the lattice mismatch for [001], [111], and [110] single quantum-well heterostructures, where the parameters of GaAs are used.

III. MECHANISM DEPENDENCE ON WHICH IS THE LEADING PARTIAL

Whether the 30° partial leads or trails the 90° partial depends upon whether the strained layer is compressive or tensile, and upon the growth direction. In the case of [001] growth, the 30° partial leads and the 90° partial trails for a compressive strained layer grown on a substrate; while in the cases of [110] and [111] growth, the 90° partial leads and the 30° partial trails for a compressive strained layer grown on a substrate. Since the glide geometry depends upon whether the 30° partial or the 90° partial is leading, the two cases are considered separately.

A. The 30° partial leading

In Fig. 1, this case corresponds to the partial A being the 30° partial and B being the 90°. As discussed above, the critical thickness of the 90° partial misfit dislocation loop is given by Eq. (7). However, when h reaches $H_c(90°,\Gamma_0)$ (the critical thickness for the 90° partial), the 90° partial moves. It is obstructed by the 30° partial, because the 30° partial is the leading partial. At each value of $h > H_c(90°,\Gamma_0)$, the 90° partial loop finds a new equilibrium position at which the excess force acting on the 90° partial loop is zero, i.e., $F_{\text{exc}(90°)}=0$. Thus, in Eq. (5a) the repulsive force acting on the 30° partial for each value of h can be obtained from $F_{\text{exc}(90°)}=0$ which gives

$$F_r = F_{\varepsilon(90°)} - F_{1(90°)} + F_s \ . \tag{8}$$

Eventually, the critical thickness for the 30° partial is reached. The critical thickness of the 30° partial loop generation can be obtained by replacing F_r in Eq. (5a) by the value given in Eq. (8), which gives

$$H_c(30°,\Gamma) = \frac{[K(90°)+K(30°)]b_p}{2\pi M[\cos\theta_{1(90°)}+\cos\theta_{1(30°)}]\varepsilon} \times \ln\left[\frac{\alpha H_c(30°,\Gamma)}{b_p}\right] . \tag{9}$$

It is noted, from Eq. (9), that the critical thickness of the 30° partial is independent of the stacking fault energy and the dissociation width.

Assuming that $\varepsilon=f$, for [001] growth direction, $H_c(90°,\Gamma_0)$ given by Eq. (7), and $H_c(30°,\Gamma)$ given by Eq. (9) are plotted in Fig. 3 as a function of f, where the same parameters for plotting Fig. 2 are used. Since $H_c(30°,\Gamma) > H_c(90°,\Gamma_0)$, the curve for $H_c(30°,\Gamma)$ corresponds to the critical thickness for the motion of the 60° dissociated threading dislocation with the 30° partial leading. For comparison, the critical thickness of a 60° perfect misfit dislocation loop generation [marked as $H_c(60°,0)$] given by Eq. (7) (with $b_p=b$ and $\theta=\theta_1=60°$) is also plotted. Figure 3 shows that $H_c(30°,\Gamma) < H_c(60°,0)$, which implies that the model of misfit dislocation loop generation from dissociated dislocations is more likely. A similar analysis for [110] and [111] growths shows that this result also applies to both of these cases. As a result of this analysis, the generation mechanism of a misfit dislocation loop from a dissociated threading dislocation with the 30° partial leading is shown schematically in Fig. 4.

B. The 90° partial leading

This case corresponds to partial A (in Fig. 1) being the 90° partial and B being the 30° partial. The critical thickness of the 90° partial misfit dislocation is given by Eq.

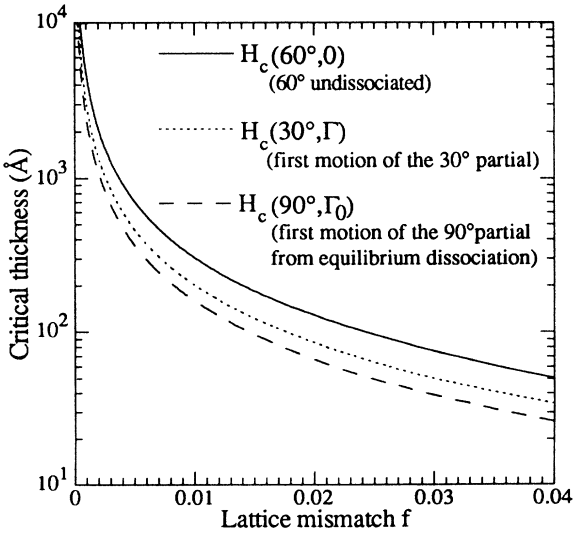

FIG. 3. Plots of the critical thicknesses of the 60° perfect misfit dislocation, the 60° dissociated misfit dislocation, and the 90° partial misfit dislocation as a function of the lattice mismatch in [001] single quantum-well heterostructures, where the parameters of GaAs are used.

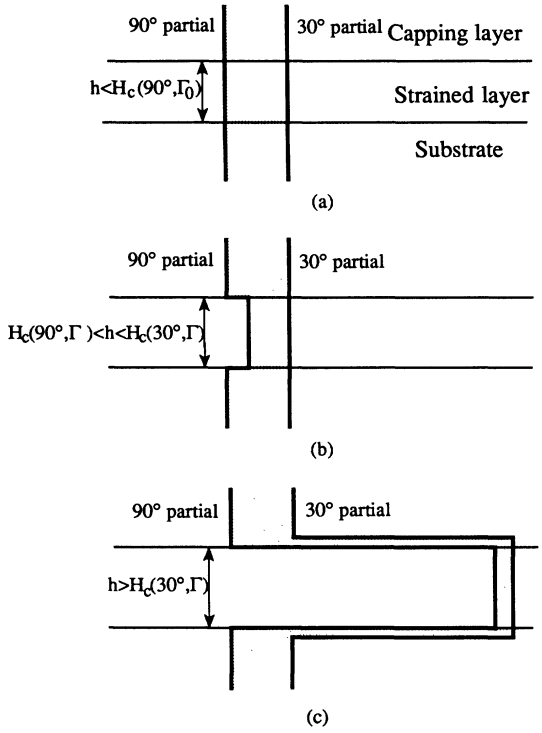

FIG. 4. Schematic diagrams of misfit dislocation generation mechanism from a dissociated threading dislocation in the case with the 30° partial leading.

(7). When h reaches $H_c(90°,\Gamma_0)$, the 90° partial moves. This causes Γ to increase beyond the equilibrium dissociation width, because as discussed above, $H_c(90°,\Gamma_0)<H_c(30°,\Gamma)$. As h is increased, Γ increases. There are then two possibilities: case 1, $H_c(30°,\Gamma)$ is reached before Γ becomes infinite, or case 2, Γ becomes infinite before $H_c(30°,\Gamma)$ is reached.

The critical thickness for the 90° partial misfit dislocation tending to move to infinity while the 30° partial remains stationary can be obtained from Eq. (6) with $\Gamma=\infty$ (and with the signs for the leading partial):

$$H_c(90°,\infty)=\frac{K(90°)b_{90°}}{2\pi\left[M\cos\theta_{1(90°)}\varepsilon-\dfrac{\gamma}{b_{90°}\cos\theta_2}\right]}\times\ln\left[\frac{\alpha H_c(90°,\infty)}{b_{90°}}\right]. \quad (10)$$

It is seen that $H_c(90°,\infty)$ depends upon the stacking fault energy. The higher the stacking fault energy, the greater is $H_c(90°,\infty)$.

Whether case 1 or case 2 applies for a particular situation depends upon whether $H_c(30°,\Gamma)$ is greater than or less than $H_c(90°,\infty)$. If $H_c(30°,\Gamma)>H_c(90°,\infty)$, case 1 applies; if $H_c(30°,\Gamma)<H_c(90°,\infty)$, case 2 applies. Therefore, the boundary between the two cases is obtained by equating Eqs. (9) and (10), which results in a *critical misfit strain*

$$\varepsilon_0=\frac{[K(30°)+K(90°)]\gamma}{Mb_p\cos\theta_2[K(30°)\cos\theta_{1(90°)}-K(90°)\cos\theta_{1(30°)}]}. \quad (11)$$

Since the misfit strain arises from the lattice mismatch f, this equation gives a *critical lattice mismatch* $f_0=\varepsilon_0$. It is noted that the critical lattice mismatch given by Eq. (11) is the same as that for the [001] single heterostructures (cf. Ref. 20), if the [001] growth direction and the isotropic formula are used. This equality is a general result, which can be obtained analytically. Since case 1 corresponds to the low strain region and case 2 corresponds to the high strain region,[20] for $f<f_0$, case 1 occurs, while for $f>f_0$, case 2 occurs.

In case 1, h increases until $H_c(30°,\Gamma)$ is reached. This is the same argument as for the case with the 30° partial leading, and so, for case with the 90° partial leading, $H_c(30°,\Gamma)$ is exactly the same as for the case with the 30° partial leading, i.e., $H_c(30°,\Gamma)$ is given by Eq. (9). Thus, for the situation where a tensile GaAs layer is sandwiched by a [001] capping layer and a [001] substrate, Fig. 3 also applies, and the same conclusion is reached, i.e., the model of the dissociated misfit dislocation loop generation is more likely.

Assuming that $\varepsilon=f$ and using $\gamma=55$ mJ/m^2 of GaAs given by Gottschalk, Patzer, and Alexander,[25] $f_0=2.2\%$ is obtained. For $f<f_0$, $H_c(90°,\Gamma_0)$ and $H_c(30°,\Gamma)$ are plotted in Fig. 5. Figure 6 shows this generation mechanism of a misfit dislocation loop from a dissociated threading dislocation for the 90° partial leading.

In case 2 (i.e., the 90° partial misfit dislocation tends to move to infinity under the excess force $F_{exc(90°)}$ before the 30° partial misfit dislocation moves), the generation mechanism from a dissociated threading dislocation is shown in Fig. 7 schematically. In this case, if h increases

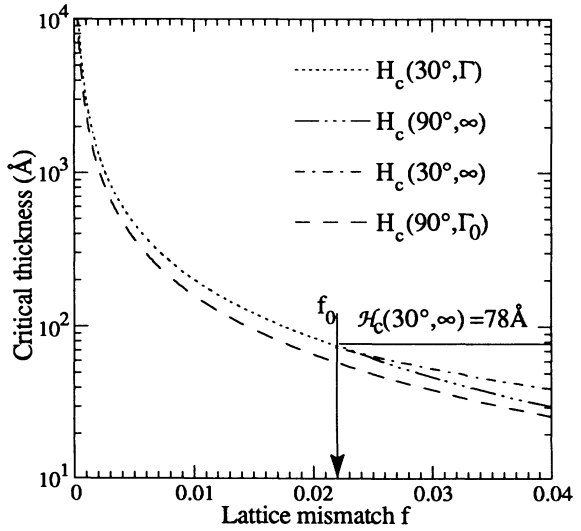

FIG. 5. Plots of the critical thicknesses against the lattice mismatch in [001] single quantum-well heterostructures with a tensile strained layer, where the parameters of GaAs are used.

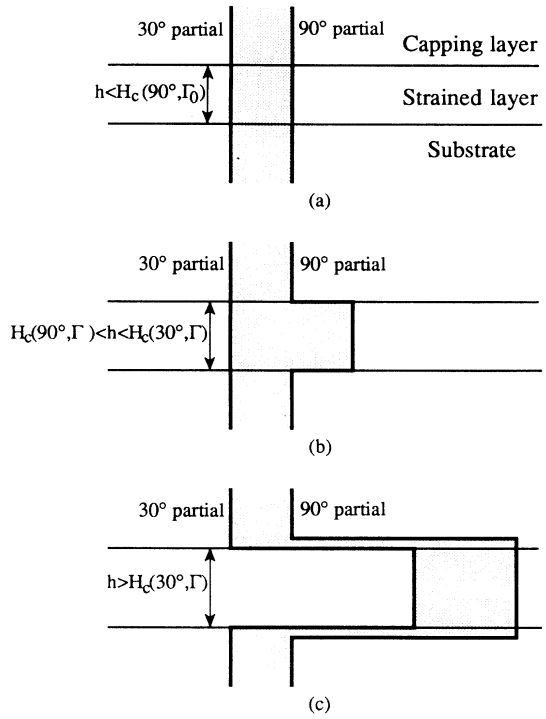

FIG. 6. Schematic diagrams of misfit dislocation generation mechanism from a dissociated threading dislocation in the case with the 90° partial leading with $f < f_0$.

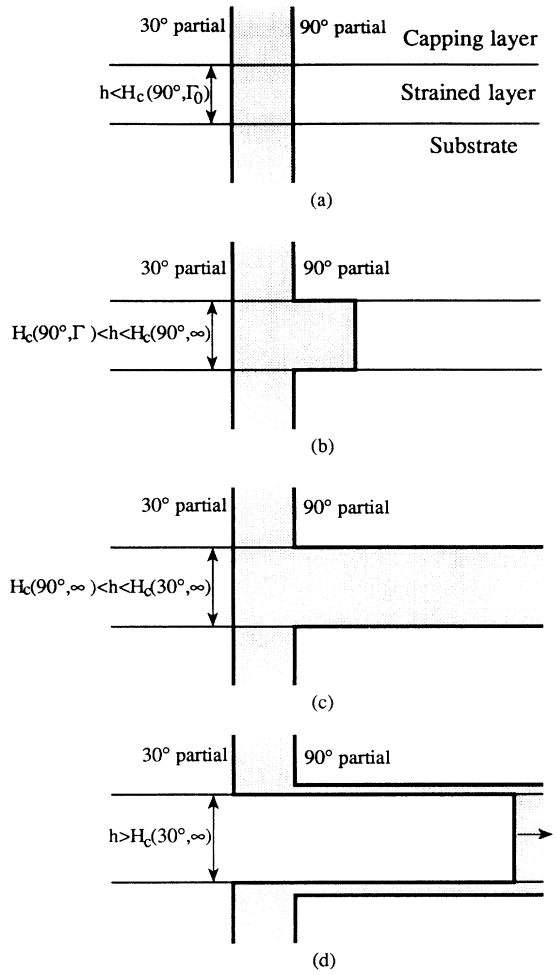

FIG. 7. Schematic diagrams of misfit dislocation generation mechanism from a dissociated threading dislocation in the case with the 90° partial leading with $f > f_0$.

above $H_c(90°, \infty)$, the situation is as in Fig. 7(c), while if $H_c(90°, \Gamma_0) < h < H_c(90°, \infty)$, Fig. 7(b) applies. As h increases, the excess force, $F_{\text{exc}(30°)}$, on the 30° partial increases, and eventually a new critical thickness for the 30° partial to move is reached. This critical thickness is given by Eq. (6) with $\Gamma = \infty$ (and with the signs for the trailing partial):

$$H_c(30°, \infty) = \frac{K(30°)b_{30°}}{2\pi\left[M\cos\theta_{1(30°)}\varepsilon + \dfrac{\gamma}{b_{30°}\cos\theta_2}\right]} \times \ln\left[\frac{\alpha H_c(30°, \infty)}{b_{30°}}\right]. \quad (12)$$

Equation (12) shows that $H_c(30°, \infty)$ depends upon the stacking fault energy. The higher the stacking fault energy, the lower is $H_c(30°, \infty)$. For $h > H_c(30°, \infty)$, Fig. 7(d) applies.

As an example, we consider the situation of the tensile strained layer and the capping layer grown on the [001] substrate. (This is the case of 90° partial leading.) For $f > f_0$ with $\varepsilon = f$, $H_c(90°, \Gamma_0)$, $H_c(90°, \infty)$, and $H_c(30°, \infty)$ are plotted in Fig. 5 where the anisotropic parameters of GaAs are used.

Figure 5 gives the misfit dislocation loop generation mechanisms for the 90° partial leading, which can be summarized as follows.

(1) For $f < f_0$ (i.e., case 1): when h reaches $H_c(90°, \Gamma_0)$, the 90° partial moves, but is obstructed by the 30° partial. Then the 90° partial will find an equilibrium position in the region of $H_c(90°, \Gamma_0) \le h \le H_c(30°, \Gamma)$. For $h \ge H_c(30°, \Gamma)$, both partials move.

(2) For $f > f_0$ (i.e., case 2): when h reaches $H_c(90°, \Gamma_0)$, the 90° partial moves and reaches an equilibrium position in the region of $H_c(90°, \Gamma_0) \le h \le H_c(90°, \infty)$; for $h \ge H_c(90°, \infty)$, the 90° partial loop tends to move to infinity; for $h > H_c(30°, \infty)$, the 30° partial moves.

It should be acknowledged that three-dimensional growth is common for lattice mismatch greater than 2%. However, whether the growth mechanism is layer by layer or three dimensional depends upon the growth conditions.[26] In fact, layer-by-layer growth can be achieved for high strained-layer heterostructures where the lattice mismatch can be greater than 2%,[26] although the possibility of cracking in high tensile strained layers must then be taken into account.[27]

IV. EFFECT OF DISSOCIATION ON ε

In the above analysis, the critical thickness of the 30° partial is determined by assuming that $\varepsilon = f$ in calculat-

ing the driving force F_ε on the 30° partial. This does not allow for the fact that the local misfit strain in the region of the 30° partial may be reduced due to the presence of the nearby 90° partial misfit dislocation loop lying in the strained interfaces. Then locally $\varepsilon < f$, and the driving force on the 30° partial will be reduced. Therefore, the practical critical thickness $H_c(30°,\Gamma)$ [or $H_c(30°,\infty)$] will be greater than the value given by Eq. (9) [or Eq. (12)].

Consider first, the case with the 30° partial leading. Since the equilibrium dissociation width of dissociated threading dislocations is very small (normally, a few tens of Å), and since the 90° partial moves but is obstructed by the 30° partial in the range $H_c(90°,\Gamma_0) < h < H_c(30°,\Gamma)$, the 90° partial can move only a short distance (in the order of a few to a few tens of Å). Then the change to the misfit strain, due to the short elongation of the 90° partial, can be ignored, i.e., the practical critical thickness for the 30° partial will be very close to $H_c(30°,\Gamma)$ given by Eq. (9).

Consider next, the two cases with the 90° partial leading. For the case in which the critical thickness for the 30° partial is reached before Γ becomes infinite, the 90° partial can move away from the 30° partial forming an extended stacking fault, but it will stop at a new equilibrium position in the range of $H_c(90°,\Gamma_0) < h < H_c(30°,\Gamma)$. The new equilibrium dissociation width can be obtained from $F_{\text{exc}(90°)}=0$, which gives

$$\Gamma = \frac{Bb_{90°}^2}{\frac{K(90°)b_{90°}^2\cos\theta_2}{2\pi h}\ln\left[\frac{\alpha h}{b_{90°}}\right]+\gamma - Mb_p\cos\theta_{1(90°)}\cos\theta_2\varepsilon} . \tag{13}$$

This equation shows that Γ depends upon the misfit strain, the stacking fault energy, the strained-layer thickness, and the growth direction. The elongation of the 90° partial will reduce the local misfit strain, and the driving force F_ε on the trailing 30° partial will be reduced. For this reason, the practical critical thickness for the 30° partial will be greater than $H_c(30°,\Gamma)$ given by Eq. (9) and the practical critical lattice mismatch will be less than f_0 as given by Eq. (11). If the elongation of the 90° partial is small (for example a few hundred Å), the local misfit strain will not change dramatically, and the changes to the misfit strain and to $H_c(30°,\Gamma)$ will be small. However, for the case in which Γ becomes infinite before the critical thickness for the 30° partial is reached, the local misfit strain may be considerably reduced due to the 90° partial elongating to infinity. Since the change to misfit strain, during the 90° partial generation, depends on the strain relaxation process case by case, it is difficult to determine the change to the misfit strain theoretically. However, a limiting case can be considered, where a sufficient number of 90° partials have moved to infinity to relax the lattice mismatch so that the system energy is a minimum. In this limiting case, for a given strained-layer thickness h [$h > H_c(90°,\infty)$], the residual misfit strain ε_c can be obtained by setting $F_{\text{exc}(90°)}=0$ with $\Gamma=\infty$, i.e.,

$$\varepsilon_c = \frac{K(90°)b_{90°}}{2\pi M\cos\theta_{1(90°)}h}\ln\left[\frac{\alpha h}{b_{90°}}\right] + \frac{\gamma}{Mb_{90°}\cos\theta_{1(90°)}\cos\theta_2} . \tag{14}$$

Thus, the driving force F_ε on the trailing 30° partial will depend on ε_c rather than on f. For this reason, the critical thickness of the 30° partial $\mathcal{H}_c(30°,\infty)$ will be given by Eq. (12) with ε being given by Eq. (14). This gives

$$\mathcal{H}_c(30°,\infty) = \frac{b_p^2\cos\theta_2[K(30°)\cos\theta_{1(90°)} - K(90°)\cos\theta_{1(30°)}]}{2\pi[\cos\theta_{1(90°)}+\cos\theta_{1(30°)}]\gamma}\ln\left[\frac{\alpha\mathcal{H}_c(30°,\infty)}{b_p}\right] . \tag{15}$$

This equation shows that the critical thickness for the 30° partial, in this limiting case, is independent of the lattice mismatch, but is dependent on the stacking fault energy and growth direction, i.e., this limiting critical thickness for the 30° partial will be a constant for a given heterostructure. The higher the stacking fault energy, the lower will be the limiting critical thickness. For GaAs with [001] growth, $\mathcal{H}_c(30°,\infty)=78$ Å, which is plotted in Fig. 5. From Fig. 5, it is seen that the value of $\mathcal{H}_c(30°,\infty)$ corresponds to the critical thicknesses of $H_c(90°,\infty)$ and $H_c(30°,\infty)$ when $f=f_0$. The two limiting critical thicknesses for the 30° partial can be understood as follows: for no misfit relaxation, the critical thickness for the 30° partial will be $H_c(30°,\infty)$ given by Eq. (12); for equilibrium misfit relaxation, the critical thickness for the 30° partial will be $\mathcal{H}_c(30°,\infty)$ given by Eq. (15); while for a partly relaxed system, the critical thickness for the 30° partial will be between $H_c(30°,\infty)$ and $\mathcal{H}_c(30°,\infty)$.

V. SOURCE OF DISLOCATIONS IN QUANTUM-WELL HETEROSTRUCTURES

A long-standing difficulty with models of layer-by-layer epitaxial growth of strained-layer quantum-well heterostructures, which involve generation of misfit dislocations loop from threading dislocations, has been that $H_c > h_c$ (h_c is the critical thickness for the misfit dislocation generation in single heterostructures). As a result, if the strained layer is grown to a thickness $h > H_c$ on the sub-

strate, then the theories (for example Ref. 3) predict that the threading dislocations will be fully extended in the strained interface before the capping layer is grown. Consequently, there is no opportunity for the model discussed in Secs. II–IV to occur. However, earlier studies[21,22] have shown that, for a strained layer grown on a substrate with $h \geq h_c$, (1) not all threading dislocations elongate in the substrate interface, and (2) the length of the misfit dislocation varies from dislocation to dislocation within the same heterostructure. The first of these observations was explained in terms of the different extents of pinning of threading dislocation during growth; the second observation is explained in terms of the activation energy of kink formation controlling misfit dislocation elongation velocities. Both of these observations indicate that the critical thicknesses predicted by the theories (for example Ref. 3) are a necessary, but not a sufficient, condition for misfit dislocations to form. In the model of misfit dislocation loop generation in quantum-well heterostructures discussed in Secs. II–IV, the misfit dislocation loops are considered to be generated from dissociated threading dislocations. The observations described above demonstrate that such dislocations are present in the single quantum-well heterostructures.

The analysis of Secs. II–IV considers the case starting with the threading dislocation segment in the strained layer having the equilibrium dissociation width. The reason for taking this starting point is to determine which is the first partial to move, and its critical thickness. However, as discussed in our previous study,[20] the dissociation width between the two partials in the strained layer, when the capping layer is grown, can be different from the equilibrium dissociation width, if the threading dislocation is elongated during the growth of the strained layer. As a consequence, the critical thickness for the 90° partial cannot be calculated using Eq. (7). However, since the 30° partial is the second to move, the critical thickness for the 30° partial will be given by Eq. (9).

VI. EXPERIMENTAL EVIDENCE

The analysis discussed in Secs. II–IV can be compared with the observations of Hwang and coworkers,[18,19,28–30] who reported the existence of stacking faults and microtwins in $InP/In_xAl_{1-x}As/In_{0.53}Ga_{0.47}As$ ($x=0.38$, 0.23, and 0) [001] quantum-well heterostructures.[18,19,28–30] They observed that these stacking faults and microtwins were contained within the strained layer, and that the stacking faults were terminated at the bounding strained interfaces by partial dislocations of the type $a\langle 112\rangle/6$. The partials at either ends of the stacking fault had opposite Burgers vectors.

Their explanation was that these partials arose from the generation of a pair of partial dislocations of the $a\langle 112\rangle/6$ type with antiparallel Burgers vectors inside the embedded strained layer, and that these partials glided to the opposite interfaces, leaving a stacking fault behind. A series of these can combine to form microtwins. Their analysis showed that the resulting pair of 90° partials is energetically preferred to the introduction of 60° perfect dislocations at the interfaces. Using the parameters given by Hwang and co-workers ($\alpha=4$, $\mu=4.7\times10^{10}$ N/m^2, $\nu=0.25$, and $\gamma=50$ mJ/m^2),[18,19] their analysis is plotted in Fig. 8, in the same way as they have plotted it, i.e., in the isotropic form. Figure 8 shows that, above a particular lattice mismatch ($f_p=0.7$ for their heterostructures), strain relief by the 90° partial misfit dislocations is preferred energetically to strain relief by undissociated 60° misfit dislocations. They did not, however, consider the possibility of the dissociated 60° dislocation discussed in this paper. The critical thickness for the 60° dissociated dislocation is also plotted in Fig. 8 using Eq. (9) (but in the isotropic form). It shows an intersection point ($f_0=1.7\%$) between the curves for the critical thicknesses for the 60° dissociated dislocation [$H_c(30°,\Gamma)$] and that for the 90° partial tending to move to infinity [$H_c(90°,\infty)$]. As discussed above, below f_0 the misfit dislocation configurations of Fig. 6 will be preferred, while above f_0 the configurations of Fig. 7 will be preferred. The experimental points of Hwang *et al.*[19] are plotted in Fig. 8. For $f=1\%$, our analysis shows that the material will have no misfit dislocations, in agreement with the experimental point. For $f=2\%$, our analysis gives $H_c(90°,\Gamma_0)=59$ Å, $H_c(90°,\infty)=71$ Å, $H_c(30°,\infty)=79$ Å, and $\mathcal{H}_c(30°,\infty)=90$ Å. This means that the 90° partial will move and extend the stacking fault width, when h reaches 59 Å; above 71 Å, the 90 Å partial moves to infinity and creates an extended stacking fault, while the 30° partial remain stationary until h reaches the practical critical thickness for the 30° partial. For $h>90$ Å, the 30° partial moves, creating dissociated 60° misfit dislo-

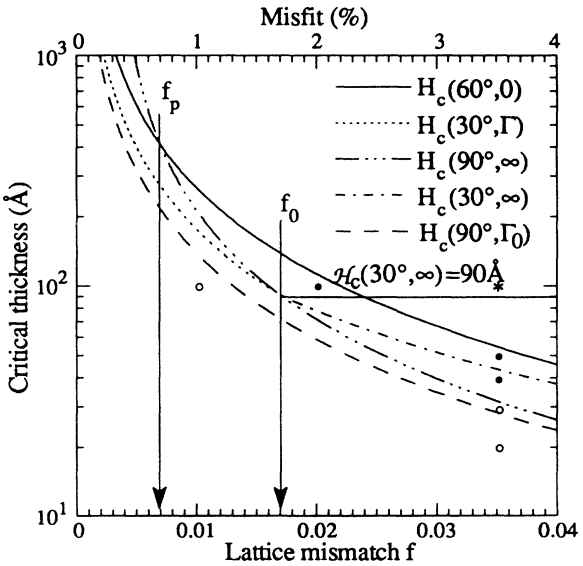

FIG. 8. The plots of the critical thicknesses as a function of f in [001] single quantum-well heterostructures with a tensile strained layer, where the parameters given by Hwang *et al.* (Ref. 18) are used. The experimental points given by Hwang *et al.* (Ref. 18) are shown in this figure, where ○ corresponds to the observation of the defect free material, ● indicates the observation of extended stacking faults, and * corresponds to the observation of heavily faulted material.

cations in each interface. The experimental point at $f=2\%$ is for extended faults at $h=100$ Å. Although this is greater than the $\mathcal{H}_c(30°,\infty)=90$ Å predicted limit for the 30° partial to move (i.e., below 90 Å, extended stacking faults are predicted), it is close to that value, and the discrepancy can be explained by the kinetics of strain relaxation processes (the excess force on each partial and the activation energy of kink formations of each partial) or other nonequilibrium effects. For $f=3.5\%$, our analysis shows that $H_c(90°,\Gamma_0)=28$ Å, $H_c(90°,\infty)=32$ Å, $H_c(30°,\infty)=44$ Å, and $\mathcal{H}_c(30°,\infty)=90$ Å. The experimental points for the defect-free material ($h=20$ and 30 Å) are less than the critical thickness for the 90° tending to infinity [$H_c(90°,\infty)=32$ Å], and are in excellent agreement with our analysis. The experimental points ($h=40$ and 50 Å) are experimental observations of extended stacking faults. These values of h are in our predicted range of the 90° partial tending to infinity [$H_c(90°,\infty)=32$ Å] with the 30° partial remaining stationary [$H_c(30°,\infty)=44$ Å$\sim\mathcal{H}_c(30°,\infty)=90$ Å], and are in excellent agreement with our analysis. The last experimental point ($h=100$ Å) reports observations of numerous stacking faults. According to our analysis, above $\mathcal{H}_c(30°,\infty)=90$ Å, both the 90° partial and the 30° partial will have extended. However, in the range of 44 to 90 Å, both 90° partial misfit dislocations, associated stacking faults, and 60° misfit dislocations will exist, the relative proportions of which will depend on kinetic arguments (the excess force on each partial and the activation energy of kink formations of each partial). This range is very close to the experimental point.

VII. MULTIPLE-QUANTUM-WELL HETEROSTRUCTURES

Consider a multiple-quantum-well heterostructure, which consists of alternating layers of B/A_xB_{1-x} (AB is used to describe an A_xB_{1-x} layer) grown epitaxially on the B substrate with layer stacking sequence of $BABBABBAB\ldots BAB/B$ as shown in Fig. 9, where the layer B and the layer AB have their own uniform layer thicknesses d_B and d_{AB}, respectively, and d_{AB} is sufficiently large to allow the dissociated misfit dislocation loop generation at both strained interfaces. If such a multiple quantum well is free of the effect of the substrate,[4,31–33] the misfit strain ε' in the coherent limit ($\varepsilon'=f'$) is[32,33]

$$\varepsilon'=f'=\frac{|a_{AB}-a_B|}{\sqrt{a_{AB}a_B}} . \tag{16}$$

For the layers B and AB, the sum of their misfit strains f_B and f_{AB} must be f' and they are[32,33]

$$f_B=\frac{Y_{AB}f'd_{AB}}{Y_{AB}d_{AB}+Y_Bd_B} \text{ and } f_{AB}=\frac{Y_Bf'd_B}{Y_{AB}d_{AB}+Y_Bd_B} , \tag{17}$$

where $Y_i=2\mu_i(1+\nu_i)/(1-\nu_i)$ is the elastic coefficient. If $Y_{AB}=Y_B$ is assumed, the simplified equations are

$$f_B=\frac{f'd_{AB}}{d_{AB}+d_B} \text{ and } f_{AB}=\frac{f'd_B}{d_{AB}+d_B} . \tag{18}$$

For the situation of $d_B\gg d_{AB}$, one obtains $f_{AB}\approx f_0$ and $f_B=0$. If the heterostructure has only two layers, this situation corresponds to a single heterostructure where a thin epitaxial layer is grown on a very thick substrate. If $d_B=d_{AB}$, then $f_{AB}=f_0/2$ and $f_B=f_0/2$. This case has been considered previously.[4]

If a threading dislocation passes through the multiple quantum wells, it can elongate in the interfaces within the multiple quantum wells to relieve the internal misfit strains when $d_{AB}>H_c(90°,\Gamma_0)$. For a threading dislocation bent over at the interfaces of an AB layer, where the AB layer is sandwiched by the layers B (see Fig. 9) and assuming $d_{AB}\le d_B$ (otherwise the elongation of the dislocation in the B layer is treated similarly), the driving force given by Eq. (1) is modified to be

$$F_\varepsilon=Mf_{AB}b_p\cos\theta_1 h . \tag{19}$$

The theoretical considerations of Secs. II–IV can then be used. For this reason, the theoretical predictions of critical thicknesses of dissociated misfit dislocations in multiple quantum-well heterostructures can be obtained from the analysis for the single quantum-well heterostructures by replacing f with f_{AB} in Eqs. (8)–(15).

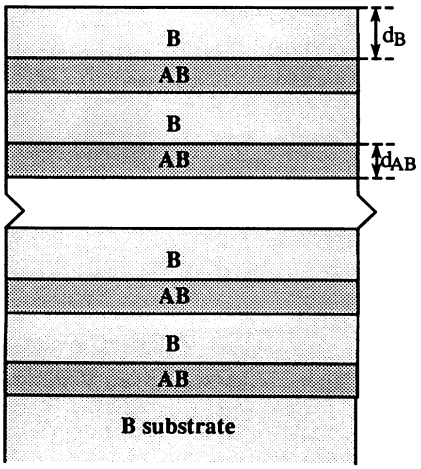

FIG. 9. Schematic diagram of a multiple quantum-well heterostructures.

VIII. CONCLUSIONS

The model reported here compares the critical thicknesses of misfit dislocation loops generated by dissociated and undissociated dislocations. It shows that the model of misfit dislocation loop generation by dissociated dislocations is more likely. The misfit dislocation generation mechanisms by the movement of dissociated dislocations are as follows:

For the 30° partial leading, above $h=H_c(90°,\Gamma_0)$, the 90° partial moves, but is obstructed by the 30° partial. For $h>H_c(30°,\Gamma)$, both partials elongate at both strained interfaces. For this reason, $H_c(30°,\Gamma)$ given by Eq. (9) is taken to be the critical thickness of misfit dislocation loop

generation by dissociated dislocations in single quantum-well heterostructures.

For the 90° partial leading, the 90° partial loop elongates at $h=H_c(90°,\Gamma_0)$. Two cases may occur:

For case 1 ($f<f_0$), the 90° partial loop reaches an equilibrium position in the region of $H_c(90°,\Gamma_0) \le h \le H_c(30°,\Gamma)$; when $h>H_c(30°,\Gamma)$, both partial loops elongate.

For case 2 ($f>f_0$), the 90° partial loop finds an equilibrium position for $h<H_c(90°,\infty)$; for $h \ge H_c(90°,\infty)$, the 90° partial loop tends to move to infinity; for $h>H_c(30°,\infty)$, the 30° partial moves. Since the 90° partial may elongate considerably (depending on f and γ) in the strained layer after $h=H_c(90°,\Gamma_0)$, $H_c(90°,\Gamma_0)$ is defined as the critical thickness of the partial misfit dislocation loop generation; for $h>H_c(30°,\Gamma)$, both partial loops elongate, so that $H_c(30°,\Gamma)$ [or $H_c(30°,\infty)$ for case 2] is defined as the critical thickness of misfit dislocation loop generation.

For multiple quantum-well heterostructures, the above arguments still apply, except with f_{AB} replacing ε in Eqs. (8)–(15).

It is evident from our previous studies[21,22] that during growth, nonequilibrium dislocation configurations exist. The model discussed in this paper applies to dislocation systems in equilibrium, and does not include the consideration of the kinetics of strain relaxation processes (for example, the effect of finite dislocation velocities). For this reason, the critical thicknesses predicted by the models discussed are only a necessary, but not a sufficient, condition for misfit dislocation generation. The effects of these kinetic strain relaxation processes and nonequilibrium configurations can only be taken into account if the model discussed in this paper is extended to include the effects of activation energies of kink formations and other nonequilibrium effects on the motions of partials, and this will be the subject of a later paper.

ACKNOWLEDGMENTS

The Australian Research Council is gratefully acknowledged for its financial support.

APPENDIX: BIAXIAL ELASTIC MODULUS IN ANISOTROPIC MEDIUM

If an anisotropic medium is considered, M depends upon the particular interface[34] and the direction in the interface. For a misfit dislocation along ⟨110⟩ direction, Nix[34] has given the biaxial elastic modulus on the (hkl) interface $M(hkl)$ as

$$M(001)=c_{11}+c_{12}-\frac{2c_{12}^2}{c_{11}},$$

$$M(110)=\frac{(c_{11}+3c_{12}+2c_{44})}{2}-\frac{(c_{11}+c_{12}-2c_{44})(c_{11}+3c_{12}-2c_{44})}{2(c_{11}+c_{12}+2c_{44})},$$

$$M(111)=\frac{6c_{44}(c_{11}+2c_{12})}{c_{11}+2c_{12}+4c_{44}},$$

where c_{11}, c_{12}, and c_{44} are the elastic constants of the strained layer. For example, if the elastic constants of GaAs are used ($c_{11}=11.88\times10^{10}$ N/m^2, $c_{12}=5.38\times10^{10}$ N/m^2, and $c_{44}=5.94\times10^{10}$ N/m^2 Ref. [35]), $M(100)=12.39\times10^{10}$ N/m^2, $M(110)=19.01\times10^{10}$ N/m^2, and $M(111)=17.39\times10^{10}$ N/m^2 can be obtained. It is seen that M varies with different interfaces. For this reason, the growth direction must be taken into account when determining F_ε. Also $\mu=4.46\times10^{10}$ N/m^2 and $\nu=0.25$ can be calculated using a Reuss average[23] and the elastic constants for GaAs given above.

[1]F. C. Frank and J. H. van der Merwe, Proc. R. Soc. London Ser. A **198**, 205 (1949); **198**, 216 (1949); **200**, 125 (1949); **201**, 261 (1950).

[2]J. H. van der Merwe, J. Appl. Phys. **34**, 117 (1963); **34**, 123 (1963).

[3]J. W. Matthews, S. Mader, and T. B. Light, J. Appl. Phys. **41**, 3800 (1970).

[4]J. W. Matthews and A. E. Blakeslee, J. Cryst. Growth **27**, 118 (1974).

[5]J. W. Matthews, J. Vac. Sci. Technol. **12**, 126 (1975).

[6]J. W. Matthews, A. E. Blakeslee, and S. Mader, Thin Solid Films **33**, 253 (1976).

[7]R. People and J. C. Bean, Appl. Phys. Lett. **47**, 322 (1985); **49**, 229(E) (1986).

[8]P. M. Maree, J. C. Barbour, J. F. van der Veen, K. L. Kavanagh, C. W. T. Bulle-Lieuwma, and M. P. A. Viegers, J. Appl. Phys. **62**, 4413 (1987).

[9]R. Hull, J. C. Bean, L. Peticolas, and D. Bahnck, Appl. Phys. Lett. **59**, 964 (1991).

[10]E. A. Fitzgerald, G. P. Watson, R. E. Proano, D. G. Ast, P. D. Kirchner, G. D. Pettit, and J. M. Woodall, J. Appl. Phys. **65**, 2220 (1989).

[11]J. H. van der Merwe and W. A. Jesser, J. Appl. Phys. **63**, 1509 (1988); **64**, 4968 (1988); Mater. Sci. Eng. A **113**, 85 (1989).

[12]B. A. Fox and W. A. Jesser, J. Appl. Phys. **68**, 2801 (1990).

[13]W. A. Jesser and B. A. Fox, J. Electron. Mater. **19**, 1289 (1990).

[14]S. C. Jain, T. J. Gosling, J. R. Willis, D. H. J. Totterdell, and R. Bullough, Philos. Mag. A **65**, 1151 (1992).

[15]T. J. Gosling, S. C. Jain, J. R. Willis, A. Atkinson, and R. Bullough, Philos. Mag. A **66**, 119 (1992).

[16]I. L. F. Ray and D. J. H. Cockayne, Proc. R. Soc. London, Ser. A **325**, 543 (1971).

[17]J. Zou and D. J. H. Cockayne, Appl. Phys. Lett. **63**, 16 (1993).

[18]D. M. Hwang, S. A. Schwarz, R. Bhat, C. Y. Chen, and T. S. Ravi, in *Gallium Arsenide and Related Compounds 1991*, edited by G. B. Stringfellow, IOP Conf. Proc. No. 120 (Institute of Physics, London, 1992), p. 365.

[19]D. M. Hwang, R. Bhat, S. A. Schwarz, and C. Y. Chen, in *Mechanisms of Heteroepitaxial Growth*, edited by B. J. Gar-

rison, R. Hull, and L. J. Schowalter, MRS Symposium Proceedings No. 263 (Materials Research Society, Pittsburgh, 1992), p. 421.
[20]J. Zou and D. J. H. Cockayne, J. Appl. Phys. **74**, 925 (1993).
[21]J. Zou, B. F. Usher, D. J. H. Cockayne, and R. Glaisher, J. Electron. Mater. **20**, 855 (1991).
[22]J. Zou, D. J. H. Cockayne, and B. F. Usher, J. Appl. Phys. **73**, 619 (1993).
[23]J. P. Hirth and J. Lothe, *Theory of Dislocations* (Wiley, New York, 1982), pp. 431, 444, and 462.
[24]W. Read, *Dislocations in Crystals* (McGraw-Hill, New York, 1953), p. 131.
[25]H. Gottschalk, G. Patzer, and H. Alexander, Phys. Status. Solidi A **45**, 207 (1978).
[26]A. Fischer-Colbrie, J. M. Miller, S. S. Laderman, S. J. Rosner, and R. Hull, J. Vac. Sci. Technol. B **6**, 620 (1988).
[27]R. M. Biefeld, C. R. Hills, and S. R. Lee, J. Cryst. Growth **91**, 515 (1988).
[28]D. M. Hwang, S. A. Schwarz, T. S. Ravi, R. Bhat, and C. Y. Chen, Phys. Rev. Lett. **66**, 739 (1991).
[29]D. M. Hwang, S. A. Schwarz, T. S. Ravi, R. Bhat, and C. Y. Chen, in *Evolution of Thin Film and Surface Microstructure,* edited by C. V. Thompson J. Y. Tsao, and D. J. Srolovitz, MRS Symposium Proceedings No. 202 (Materials Research Society, Pittsburgh, 1991), p. 531.
[30]D. M. Hwang, S. A. Schwarz, R. Bhat, C. Y. Chen, and T. S. Ravi, Opt. Quantum Electron. **23**, S829 (1991).
[31]J. P. Hirth, S. Afr. J. Phys. **9**, 72 (1985).
[32]J. P. Hirth and X. Feng, J. Appl. Phys. **67**, 3343 (1990).
[33]R. Hull, J. C. Bean, F. Cerdeira, A. T. Fiory, and J. M. Gibson, Appl. Phys. Lett. **48**, 56 (1986).
[34]W. D. Nix, Metall. Trans. A **20**, 2217 (1989).
[35]T. B. Bateman, H. J. McSkimin, and J. W. Whelan, J. Appl. Phys. **30**, 544 (1959).

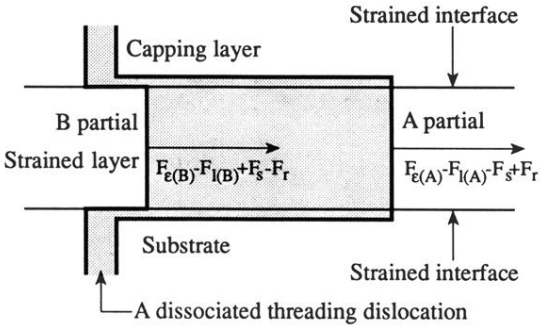

FIG. 1. Schematic diagram of the misfit dislocation generation from a dissociated threading dislocation in single quantum-well heterostructures. Four forces acting on each partial in the strained layer are shown.

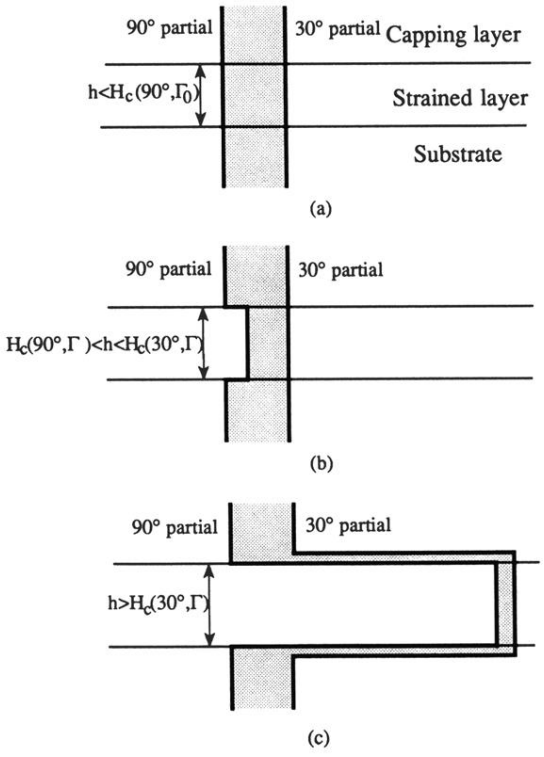

FIG. 4. Schematic diagrams of misfit dislocation generation mechanism from a dissociated threading dislocation in the case with the 30° partial leading.

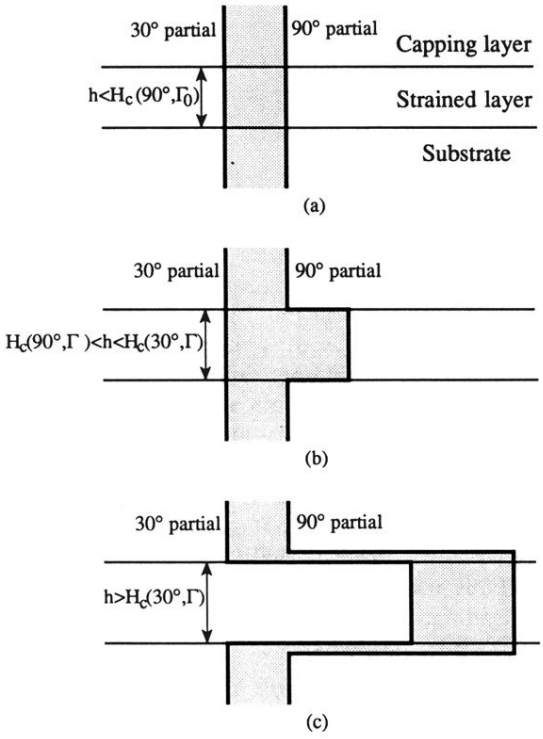

FIG. 6. Schematic diagrams of misfit dislocation generation mechanism from a dissociated threading dislocation in the case with the 90° partial leading with $f < f_0$.

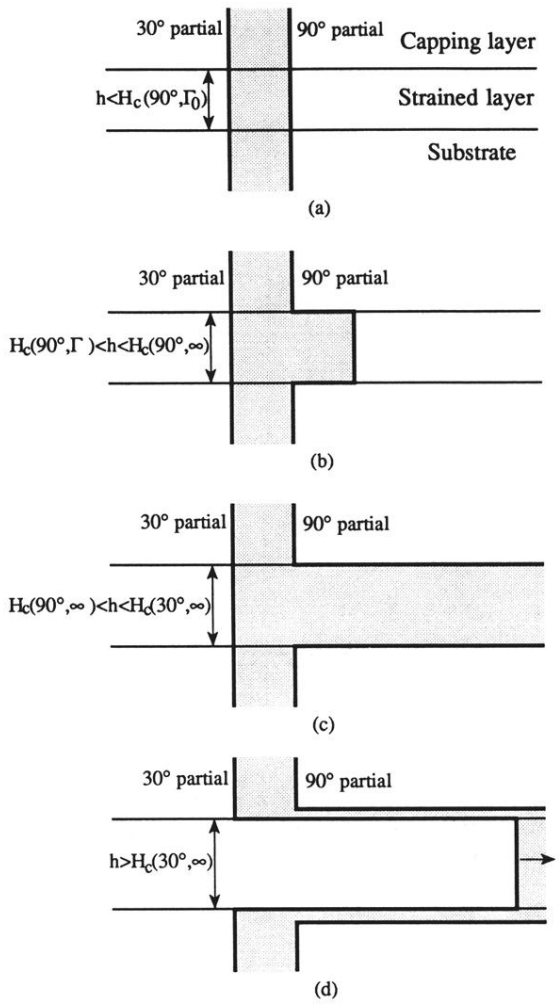

FIG. 7. Schematic diagrams of misfit dislocation generation mechanism from a dissociated threading dislocation in the case with the 90° partial leading with $f > f_0$.

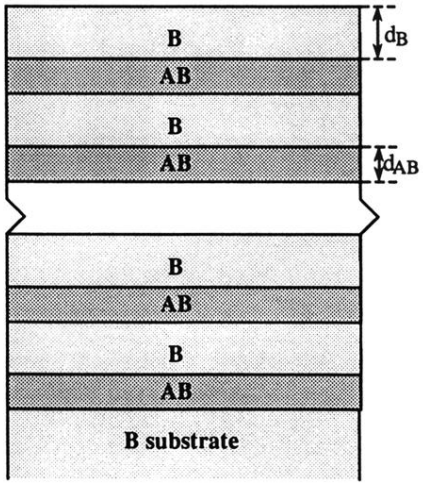

FIG. 9. Schematic diagram of a multiple quantum-well heterostructures.